



# Simulation of dark scalar particle sensitivity in $\eta$ rare decay channels at HIAF

Yang Liu (刘洋)<sup>1,2</sup> Rong Wang (王荣)<sup>1,2</sup>  Zaiba Mushtaq<sup>1,2</sup> Ye Tian (田野)<sup>1,2</sup> Xionghong He (何熊宏)<sup>1,2</sup>   
Hao Qiu (仇浩)<sup>1,2</sup> Xurong Chen (陈旭荣)<sup>1,2</sup>

<sup>1</sup>Institute of Modern Physics, Chinese Academy of Sciences, Lanzhou 730000, China

<sup>2</sup>School of Nuclear Science and Technology, University of Chinese Academy of Sciences, Beijing 100049, China

**Abstract:** The search for dark portal particles is a prominent topic at the frontier of particle physics. We present a simulation study of an experiment suitable for searching for scalar portal particles at the Huizhou  $\eta$  factory. The high-intensity proton beam from HIAF and a high event-rate spectrometer are suggested to conduct this experiment, both of which are well-suited for the discovery of new physics. Under a conservative estimation,  $5.9 \times 10^{11}$   $\eta$  events could be produced during a one-month operation of the experiment. The hadronic production of  $\eta$  mesons ( $p + {}^7\text{Li} \rightarrow \eta X$ ) was simulated at a beam energy of 1.8 GeV using the GiBUU event generator. We searched for light dark scalar particles through rare decay channels, namely  $\eta \rightarrow S\pi^0 \rightarrow \pi^+\pi^-\pi^0$  and  $\eta \rightarrow S\pi^0 \rightarrow e^+e^-\pi^0$ . The detection efficiencies of the channels and the spectrometer resolutions were studied in the simulation. We also present the projected upper limits of the decay branching ratios of the dark scalar particle and the projected sensitivities to the model parameters.

**Keywords:** super eta factory, eta rare decay, dark scalar particle, new physics

**DOI:** 10.1088/1674-1137/ad9d1b **CSTR:** 32044.14.ChinesePhysicsC.49034103

## I. INTRODUCTION

Over the past few decades, the identification of Dark Matter (DM) and Dark Energy has been among the most extensively researched topics in particle physics and astrophysics [1–5]. The Standard Model (SM) of particle physics has been tested with remarkable precision; however, it fails to explain the mechanism of DM production and its potential interactions with ordinary visible matter. In the pursuit of new physics, theoretical physicists have continually proposed innovative extensions to the SM [6–16]. Simultaneously, numerous experiments have been conducted in the hope of unraveling the mysteries of DM [17–23]. For instance, several high-energy experiments at the Large Hadron Collider have been designed to probe the interactions between DM and visible matter, with the potential to measure the properties of DM particles upon their detection [24, 25].

Among the theories proposed in the past, the Weakly Interacting Massive Particle (WIMP) has been considered one of the most promising candidates for DM [26–28]. Typically, WIMPs have a very large mass scale ( $\sim$ TeV) and interact with visible matter only through the weak interaction. However, the parameter space for WIMPs is almost experimentally excluded [18, 29–31].

Theoretically, light WIMPs (ranging from MeV to GeV) would have been produced abundantly in the early universe, unless their annihilation rates were enhanced by the simultaneous production of neutral mediator particles [6, 32, 33]. Given that light DM particles currently have few experimental constraints, they have become a key focus for future experimental searches. An increasing number of collaborations worldwide are shifting their efforts to searching for DM particles in the low-mass region [6, 7, 34, 35].

The interaction mediators in the dark sector have small masses (ranging from MeV to GeV) compared to WIMPs, making them relatively long-lived, electrically neutral vector or scalar particles [6, 32, 33]. Recently, experimental data have indicated the presence of new physics in the low-energy region around the GeV scale [36–39], which can be explained by involving interactions with invisible particles through the so-called "portal" particles [40–44]. Unlike traditional WIMPs, portal particles are not required to have a large mass or to contribute significantly to DM. Instead, portal particles serve as interaction mediators between the dark and SM sectors. They are likely new gauge particles that couple weakly with visible matter [6, 45]. According to their quantum numbers, portal particles are typically classified

Received 2 October 2024; Accepted 10 December 2024; Published online 11 December 2024

<sup>†</sup> E-mail: rwang@impcas.ac.cn

©2025 Chinese Physical Society and the Institute of High Energy Physics of the Chinese Academy of Sciences and the Institute of Modern Physics of the Chinese Academy of Sciences and IOP Publishing Ltd. All rights, including for text and data mining, AI training, and similar technologies, are reserved.

into vector portal, scalar portal, heavy lepton portal, and axion-like portal particles.

As a quasi Goldstone particle,  $\eta$  features all zero quantum numbers ( $I^G J^{PC} = 0^+ 0^+$ ). The  $\eta$  meson has a relatively small decay width, given that many strong and electromagnetic decays are forbidden at the tree level owing to the conservation of  $P$ ,  $C$ ,  $G$  parities and angular momentum. Therefore, the rare decay channels of  $\eta$  involving dark portal particles exhibit relatively large decay widths. Furthermore, the  $\eta$  meson has long been recognized as a testing ground for the violation of discrete symmetries [46]. Given that the rare decay channels of the  $\eta$  meson involve interesting physics, many experiments have already been conducted to achieve precise measurements of  $\eta$  decays, such as BESIII [47–52], KLOE/KLOE-II [53–56], and JLab Eta Factory experiments [7]. Recently, the REDTOP experiment was proposed to probe new physics via rare  $\eta$  and  $\eta'$  decays, with many more statistical metrics of the  $\eta$  yield [35]. It is suggested that the  $\eta$  meson decay is highly suitable for studying various conjectured dark portal particles that connect the SM sector with the hidden sector.

To explore new physics through rare  $\eta$  meson decays, the statistical sample of  $\eta$  mesons needs to be extremely high. Given that the hadronic production reaction of the  $\eta$  meson has a significantly large cross-section, a high-intensity proton beam is an ideal tool for generating an unprecedented number of  $\eta$  samples. Recently, it has been proposed to build a super  $\eta$  factory in Huizhou [57]. In this paper, we provide further information on the simulation of dark scalar particles at the proposed  $\eta$  factory in Huizhou, expanding on the contents presented in Ref. [57]. The High Intensity Heavy-Ion Accelerator Facility (HIAF), currently under construction in Huizhou, offers a unique opportunity to establish a super  $\eta$  factory, given that it can provide the strongest pulse intensity ion beam in its energy region. To assess the potential physics impact on dark scalar particles at the proposed Huizhou  $\eta$  factory, we conducted simulations. This paper, we present details of these simulations and the projected sensitivity to dark scalar particles in a preliminary experiment with one month of operation at the Huizhou  $\eta$  factory.

The organization of the paper is as follows. A brief review of the theoretical models of dark scalar portal particles is provided in Sec. II. The conceptual design of the spectrometer for the super  $\eta$  factory is discussed in Sec. III. The simulation framework for this study is introduced in Sec. IV. The simulation results and related discussions are presented in Sec. V. Finally, a concise summary is given in Sec. VI.

## II. THEORETICAL MODELS OF DARK SCALAR PORTAL

In scalar portal models, the dark sector couples to the

SM sector via interaction with the Higgs boson or an extension of the latter [12, 32, 58–60]. A new scalar particle is hypothesized in these models, commonly referred to as the dark scalar particle because of its coupling with the hidden dark sector. In the simulations, we focused on testing the minimal and hadrophilic scalar models, which allow the rare decay channels  $\eta \rightarrow S\pi^0 \rightarrow e^+e^-\pi^0$  and  $\eta \rightarrow S\pi^0 \rightarrow \pi^+\pi^-\pi^0$ , respectively.

### A. Minimal Scalar Model

The simplest extension of the scalar sector of the SM [11, 58, 61–63] involves introducing a single real scalar  $S$  that is a gauge singlet. As the minimum extension of the scalar field of the SM, this model is characterized by the inclusion of an additional singlet field and the presence of two types of couplings, namely  $\mu$  and  $\lambda$  [11]. At low energies, the involved dark scalar particle decays into the electron-positron pair in these models [63, 64]. Therefore, it is possible to find the signal of a light dark scalar particle in the  $\eta$  decay channel  $\eta \rightarrow S\pi^0 \rightarrow e^+e^-\pi^0$ . The SM decay of  $\eta \rightarrow e^+e^-\pi^0$  is usually described with a two-photon intermediate state to conserve  $C$  parity. The branching ratio of the SM decay  $\eta \rightarrow e^+e^-\pi^0$  is estimated to be on the order of  $10^{-9}$ , resulting in a small SM background. The relevant parameter of dark scalar particles in the  $\eta$  decay is the mixing angle  $\sin(\theta)$ , which describes the mixing effect of both the Higgs boson and the dark scalar particle. At low energies, the Higgs field can be described by  $H = (v+h)/\sqrt{2}$ , where  $v$  is the electric-weak vacuum expectation value and  $h$  is the field corresponding to the physical Higgs boson. The nonzero  $\mu$  in the dark scalar portal  $\mu S H H$  leads to small mixing between the Higgs boson and the dark scalar particle expressed as  $\theta = \mu v / (m_{\text{H}}^2 - m_S^2)$  in the small-mixing limit [6]. Following Tulin's parametrization [7, 35], the mixing angle is connected with the branching ratio of the  $\eta$  decay according to the following equation:

$$\text{Br}(\eta \rightarrow \pi^0 S) \simeq 1.8 \times 10^{-6} \lambda^{1/2} \left( 1, \frac{m_S^2}{m_\eta^2}, \frac{m_{\pi^0}^2}{m_\eta^2} \right) \sin^2 \theta, \quad (1)$$

where the mixing angle  $\theta$  is an unknown parameter and  $\lambda$  is a function related to the kinematics ( $\lambda(a, b, c) = a^2 + b^2 + c^2 - 2ab - 2ac - 2bc$ ). Note that Eq. (1) is based on a numerical and approximate evaluation with an uncertainty on the order of 20%.

### B. Hadrophilic Scalar Model

Recently, a hadrophilic (or leptophobic) scalar model was proposed. This model introduces a set of challenges, including the emergence of a new flavor-changing neutral current (FCNC) and a naturalness problem associated with the light scalar mass [13, 14]. In general, to satisfy the constraints imposed by FCNCs, the hadrophilic scal-

ar interaction must be "flavor-specific". Extensive analyses have been conducted to address these issues [13, 14]. It was found that couplings to specific quark mass eigenstates can satisfy existing FCNC constraints, even for relatively large couplings within the natural parameter space. This assumption offers a promising approach for searching for the hadrophilic scalar particle. In this study, we exclusively considered couplings to first-generation quarks. The corresponding Lagrangian is expressed as

$$\mathcal{L} \supset \frac{1}{2}(\partial_\mu S)^2 - \frac{1}{2}m_S^2 S^2 - g_u S \bar{u}u, \quad (2)$$

where  $m_h$  is the scalar mass and  $g_u$  is the effective coupling parameter to the up quark. For the hadrophilic scalar model, the branching ratio of dark scalar particle in  $\eta$  rare decay is expressed as [7, 13, 35],

$$\text{Br}(\eta \rightarrow \pi^0 S) = \frac{c_{S\pi^0\eta}^2 g_u^2 B^2}{16\pi m_\eta \Gamma_\eta} \lambda^{1/2} \left( 1, \frac{m_S^2}{m_\eta^2}, \frac{m_{\pi^0}^2}{m_\eta^2} \right), \quad (3)$$

where  $g_u$  is an unknown coupling parameter,  $B \cong m_\pi^2 / (m_u + m_d) \approx 2.6$  GeV,  $c_{S\pi^0\eta} = \frac{1}{\sqrt{3}} \cos\theta - \sqrt{\frac{2}{3}} \sin\theta$  is a parameterized coefficient used to describe the effect of  $\eta$ - $\eta'$  mixing, and  $\lambda$  is a function related to the kinematics. Owing to  $SU(3)$  breaking, the physical states of  $\eta$  and  $\eta'$  mesons are the mixed states of the singlet and octet states. To study the meson decay at the quark level, the  $\eta$ - $\eta'$  mixing angle is considered. At low energies, the interactions of dark scalar particles with pseudo Nambu-Goldstone bosons is associated with chiral symmetry breaking in terms of the known meson masses, resulting in a dimensional parameter  $B \approx m_\pi^2 / (m_u + m_d)$  [13].

### III. A COMPACT SILICON-PIXEL-BASED SPECTROMETER

The conceptual design of the spectrometer for the super  $\eta$  factory experiment is shown in Fig. 1, which includes the main parts. The tracking system is entirely based on silicon pixel detectors with a small position resolution of approximately 10  $\mu\text{m}$ . It includes forward parallel plate modules spaced 10 cm apart and central barrel modules with 5 cm gaps. The high event-rate capacity of the system is achieved through a dual-readout technique that records both the arrival time and the deposited energy in each pixel. The time-of-flight (TOF) detector is composed of low-gain avalanche detectors (LGADs) with a low material budget, serving as the primary particle identification system for low-energy particles. The outer layer of the TOF detector measures 100 cm in length and has a radius of 30 cm. Surrounding the TOF detector is the electromagnetic calorimeter (EMC), constructed from radiation-hard lead glass for high-energy photon detec-

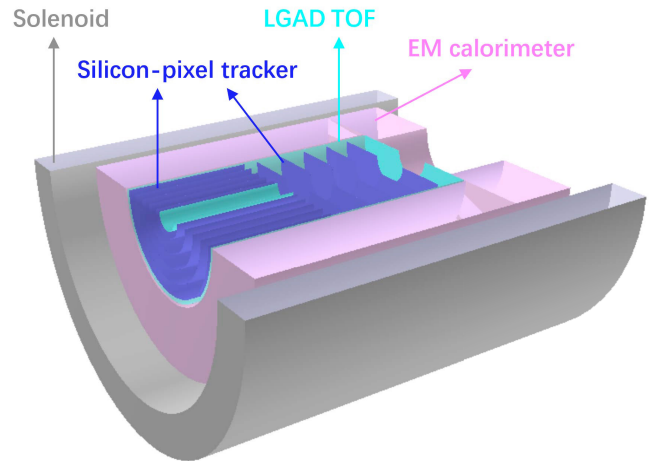


**Fig. 1.** (color online) Conceptual design of a compact spectrometer for the  $\eta$  rare decay experiment. The grey, magenta, cyan, and blue modules correspond to the solenoid, EM calorimeter, TOF detector, and silicon-pixel tracker, respectively.

tion. The fast time response of Cerenkov light in lead glass supports the high event rate of the EMC. Furthermore, the significant suppression of neutron background is attributed to the minimal Cerenkov light produced in hadronic showers. Our Geant4 simulations suggest that low-energy neutron background can be effectively neglected in the lead-glass EMC. All the key detectors mentioned are housed within a superconducting solenoid, enabling precise momentum measurement of charged particles.

Thanks to the small position resolution and high event-rate capacity of the silicon pixel detector, the spectrometer was designed to be compact, with a solenoid inner radius of approximately 60 cm. Multi-layer thin foil targets composed of light nuclei are positioned near the entrance of the spectrometer, thereby maximizing the acceptance of forward particles in the fixed-target experiment. The momentum and angular distributions of the final-state particles from the targeted  $\eta$  decay channels are shown in Figs. 2 and 3. The momentum and angular distributions of the reconstructed final-state particles from the detector simulation are also presented in the figures. The results indicate that the majority of the final-state particles can be effectively measured with the currently designed spectrometer.

### IV. SIMULATION FRAMEWORK

For  $\eta$  meson production in proton-nucleus collisions, we used the Giessen Boltzmann-Uehling-Uhlenbeck (GiBUU) event generator. This generator is based on the Boltzmann and Uehling-Uhlenbeck equations [65–67], enabling the study of particle interactions and transport processes in a nuclear environment. Interactions, collisions, and scattering processes between nucleons were in-

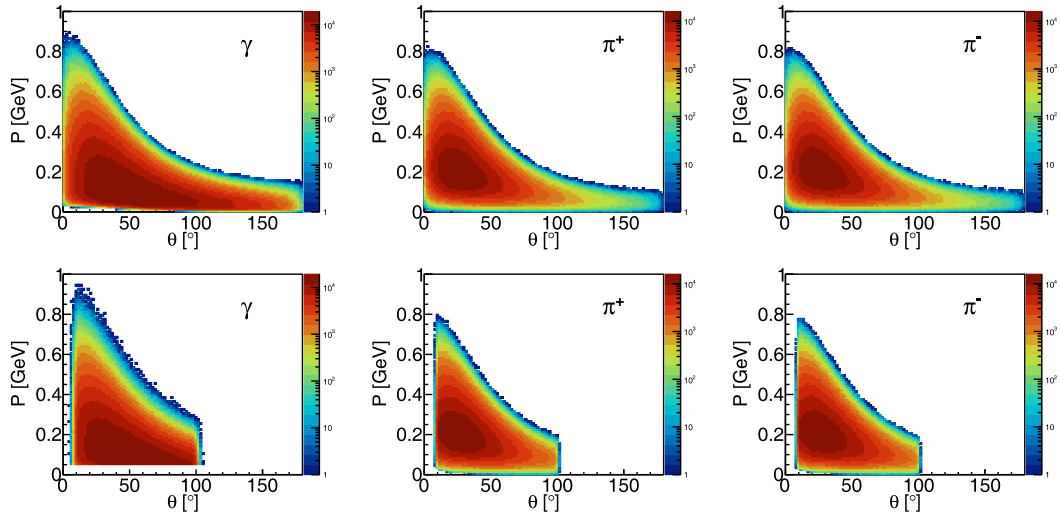


**Fig. 2.** (color online) Momentum versus angle distributions of the final-state particles from the decay channel  $\eta \rightarrow \pi^+\pi^-\pi^0(\gamma\gamma)$ .

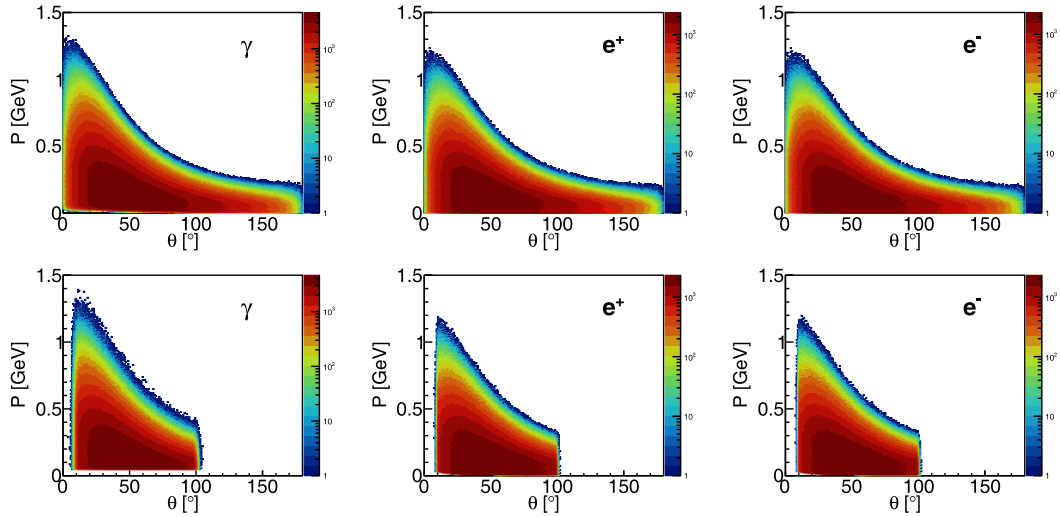


**Fig. 3.** (color online) Momentum versus angle distributions of the final-state particles from the decay channel  $\eta \rightarrow e^+e^-\pi^0(\gamma\gamma)$ .

incorporated using the Monte Carlo (MC) method for numerical solutions. The GiBUU generator is versatile, capable of describing various nuclear physics phenomena over energies ranging from 100 MeV to 100 GeV, including heavy-ion collisions, nuclear reactions, and nuclear structure studies. Following the  $\eta$  meson production modeled by the GiBUU event generator, we programmed specific decay chains of the  $\eta$  meson to ensure more realistic simulations. This approach also allowed us to evaluate the efficiency and resolution of the channels of interest.

For the spectrometer simulation, we constructed the ChnsRoot package, which is based on the FairRoot framework [68]. The FairRoot framework provides the core services for detector simulation and offline analysis, allowing users to quickly and conveniently construct experimental setups. In ChnsRoot, we implemented a fast simulation based on Geant4 simulation results, focusing

on the energy resolutions and efficiencies of the detectors. Using the ChnsRoot package, we efficiently and reliably studied the acceptances, efficiencies, and resolutions of the detectors.

The angular acceptances of both charged and neutral particles were designed to be in the range from  $10^\circ$  to  $100^\circ$  in the conceptual design of the spectrometer. [Figures 2 and 3](#) show the reconstructed kinematics from the ChnsRoot simulations for pions, electrons, and photons in the studied  $\eta$  decay channels. The minimum momentum of charged particles is constrained by the inner radius of the silicon pixel tracker. For neutral particles, the hit threshold of the EMC was set to the value induced by a 50 MeV photon. According to these simulations, this EMC threshold effectively rejects the low-energy neutron background while preserving as many photons as possible.

The statistics of the  $\eta$  meson samples are a crucial in-



put for both future experiments and the simulations presented in this study. The statistics depend on several factors, including the energy setting, cross-section, and running time of future experiments. The proton beam energy was set at 1.8 GeV, just below the  $\rho$  production threshold, to minimize background. At this energy, the probability of  $\eta$  production in elastic scattering is approximately 0.76%, as derived from the GiBUU simulation of p- $^7\text{Li}$  collisions. Extrapolating from previous measurements, the  $\eta$  production cross section in p-p collisions is approximately 0.1 mb at 1.8 GeV [69]. Thus, the cross-section in  $p\text{-}A$  collisions is approximately  $0.1 \times A$  mb. The multi-layer target of thin foils (lithium or beryllium) will be used in future experiments. The luminosity of the fixed target experiment can reach  $10^{35} \text{ cm}^{-2}\text{s}^{-1}$ . A light nuclear target is used to reduce both the background and particle multiplicity. However, considering the event rate capacity of the spectrometer, we assume a conservative event rate of inelastic scattering at 100 MHz. For a conservative estimation of the impact of the future experiment, we assume that the experiment will run for one month with a duty factor of 30%. Based on this, we estimate that the number of  $\eta$  mesons produced in a future preliminary experiment will be  $5.9 \times 10^{11}$ .

In this study, we simulated approximately 13 million inelastic p-A collision events owing to limitations in computing resources and storage capacity. To predict the sensitivity of a real experiment, we scaled up both the background distributions and the number of produced  $\eta$  samples accordingly, using a scaling factor of approximately  $10^5$ . The total number of events in the future  $\eta$  factory experiment is expected to reach a spectacular scale.

## V. RESULTS AND DISCUSSION

From MC simulations, we estimated the detection efficiencies of the channels of interests. Next, we show the resolutions of the masses of  $\pi^0$ ,  $\eta$ , and dark scalar particles. We also report on the projected background distributions after applying the event selection criteria. We computed the upper limits of branching ratios of the studied channels. Finally, the sensitivities of the model parameters were obtained from the simulation data.

### A. Efficiencies

The detection efficiencies for the targeted  $\eta$  decay channels are crucial for optimizing the design of the spectrometer. The input MC and reconstructed events are shown in Figs. 4 and 6 for the channels  $\eta \rightarrow \pi^0 e^+ e^-$  and  $\eta \rightarrow \pi^0 \pi^+ \pi^-$ , respectively. The detection efficiencies as a function of the dark scalar mass (invariant mass of its decay products) are shown in Figs. 5 and 7. It can be seen that the efficiencies exceed 40% for both channels targeted for dark scalar particle exploration. These efficiencies are satisfactory, given that they are very close to the

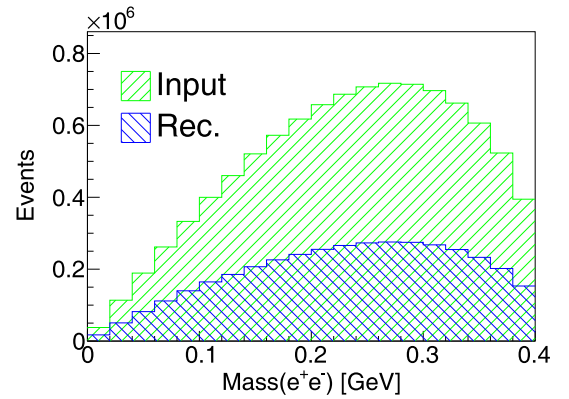


**Fig. 4.** (color online) Event distributions as a function of the mass of the dark scalar particle for the channel  $\eta \rightarrow \pi^0 e^+ e^-$ . The green and blue histograms show the input MC events from the event generator and the reconstructed events from the detector simulation, respectively.

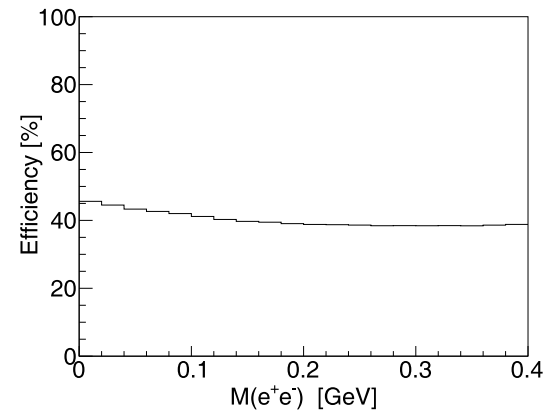


**Fig. 5.** Collecting efficiency of the channel  $\eta \rightarrow \pi^0 e^+ e^-$  as a function of  $M(e^+ e^-)$ .

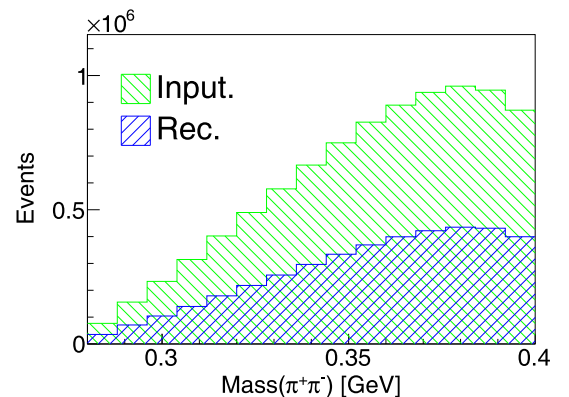


**Fig. 6.** (color online) Event distributions as a function of the mass of the dark scalar particle for the channel  $\eta \rightarrow \pi^0 \pi^+ \pi^-$ . The green and blue histograms show the input MC events from the event generator and the reconstructed events from the detector simulation, respectively.

pure geometrical acceptances.

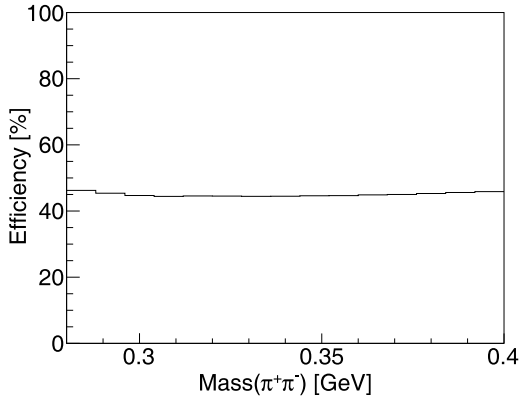


**Fig. 7.** Collecting efficiency of the channel  $\eta \rightarrow \pi^0 \pi^+ \pi^-$  as a function of  $M(\pi^+ \pi^-)$ .

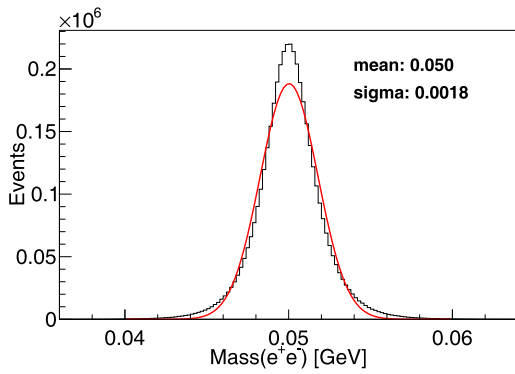


**Fig. 8.** (color online) Invariant mass distribution of  $e^+ e^-$  from the dark scalar decay channel  $\eta \rightarrow S \pi^0 \rightarrow e^+ e^- \gamma \gamma$ . The mass of the dark scalar particle was assumed to be 50 MeV in this simulation.

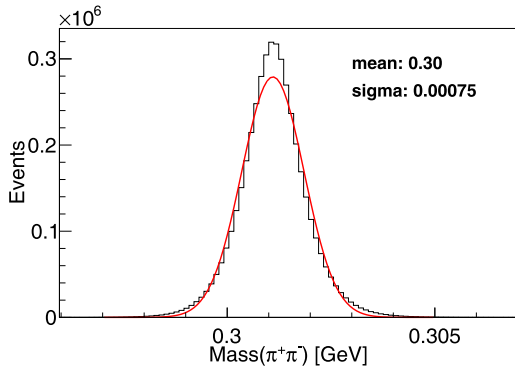


**Fig. 9.** (color online) Invariant mass distribution of  $\pi^+ \pi^-$  from the dark scalar decay channel  $\eta \rightarrow S \pi^0 \rightarrow \pi^+ \pi^- \gamma \gamma$ . The mass of the dark scalar particle was assumed to be 300 MeV in this simulation.

### B. Invariant mass resolutions

In the simulation, we programmed the following decay chains of  $\eta$  meson decay with a presumed dark scalar particle:  $\eta \rightarrow S \pi^0 \rightarrow e^+ e^- \gamma \gamma$  and  $\eta \rightarrow S \pi^0 \rightarrow \pi^+ \pi^- \gamma \gamma$ . From the ChnsRoot simulations, the distributions of the recon-

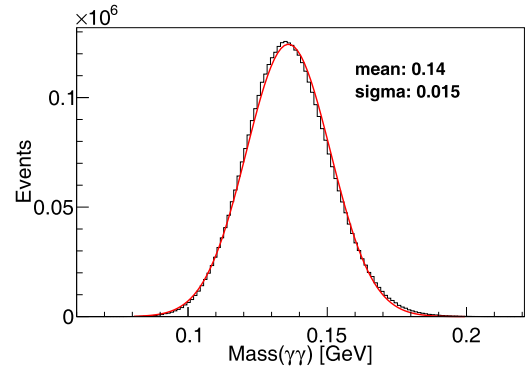


**Fig. 10.** (color online) Distribution of the reconstructed  $\pi^0$  mass from the channel  $\eta \rightarrow e^+ e^- \pi^0 \rightarrow e^+ e^- \gamma \gamma$ .

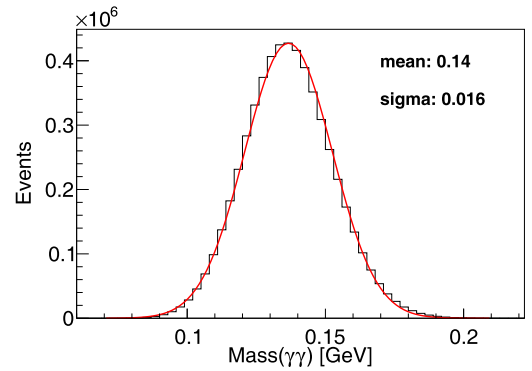


**Fig. 11.** (color online) Distribution of the reconstructed  $\pi^0$  mass from the channel  $\eta \rightarrow \pi^+ \pi^- \pi^0 \rightarrow \pi^+ \pi^- \gamma \gamma$ .

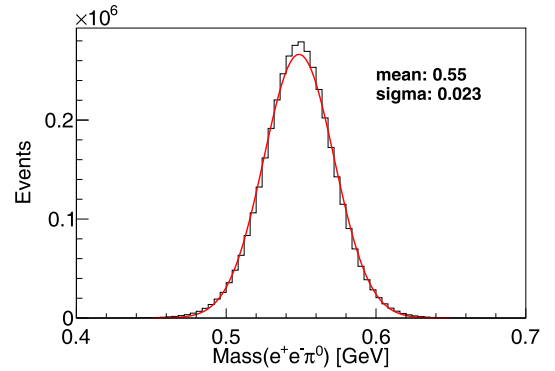


**Fig. 12.** (color online) Distribution of the reconstructed  $\eta$  mass from the channel  $\eta \rightarrow e^+ e^- \pi^0$ .

structed mass of the dark scalar particle are shown in Figs. 8 and 9 for  $e^+ e^-$  and  $\pi^+ \pi^-$  channels, respectively. Thanks to the small spatial resolution of the silicon pixel detector, the mass resolution for the dark scalar particle is also very small, less than 2 MeV for both channels. This small mass resolution is crucial for the sensitivity to new particles, given that it reduces the number of background events under the narrower peak.

For the event selection, we also needed to identify  $\pi^0$  and  $\eta$  particles from the invariant mass distributions. Based on the ChnsRoot simulations, the distributions of

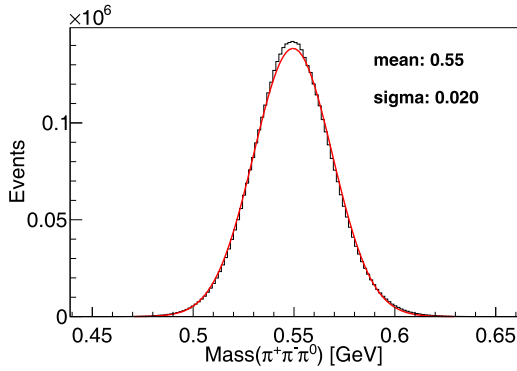


**Fig. 13.** (color online) Distribution of the reconstructed  $\eta$  mass from the channel  $\eta \rightarrow \pi^+\pi^-\pi^0$ .

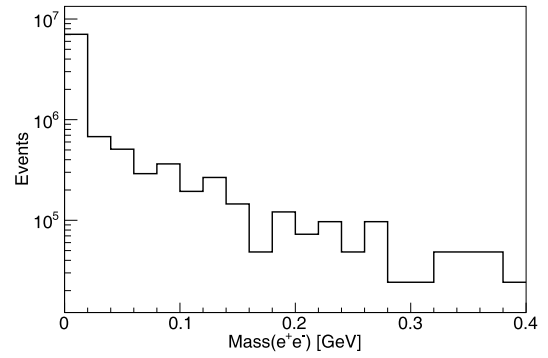


**Fig. 14.** Projected invariant mass distribution of  $e^+e^-$  in the channel  $\eta \rightarrow e^+e^-\pi^0$  for the suggested one-month running experiment.

the reconstructed mass of the decay  $\pi^0$  are shown in Figs. 10 and 11 for  $e^+e^-\pi^0$  and  $\pi^+\pi^-\pi^0$  channels, respectively. According to the current design of the EMC, the mass resolution of  $\pi^0$  is not as good as expected, being approximately 15 MeV for both  $\eta$  decay channels. The distributions of the reconstructed mass of the  $\eta$  meson are shown in Figs. 12 and 13 for  $e^+e^-\pi^0$  and  $\pi^+\pi^-\pi^0$  channels, respectively. According to our simulations, the mass resolution of the  $\eta$  meson is approximately 20 MeV for both studied decay channels. The resolution of the  $\eta$  mass mainly comes from the resolution of  $\pi^0$ , given that our designed spectrometer excels in measuring the momentum of charged particles accurately. Small mass resolution enables the application of strict criteria for  $\pi^0$  and  $\eta$  selections, thereby reducing the background and improving the sensitivity to dark scalar particles. Improving the energy resolution of the EMC is an effective approach for improving the resolutions of the masses of  $\pi^0$  and  $\eta$ .

### C. Background distributions

The targeted decay channels of  $\eta$  for searching for dark scalar particles are  $\eta \rightarrow e^+e^-\pi^0$  and  $\eta \rightarrow \pi^+\pi^-\pi^0$ . The technique to find dark scalar particles consists in searching for a bump in the invariant mass distributions of  $e^+e^-$  and  $\pi^+\pi^-$ . Before generating the targeted invariant mass distributions, we selected the channels of interests. The reconstructed masses of  $\eta$  and  $\pi^0$  were required to be within the  $\pm 3\sigma$  range.

Figures 14 and 15 show the simulated invariant mass distributions of  $e^+e^-$  and  $\pi^+\pi^-$  from the channels  $\eta \rightarrow e^+e^-\pi^0$  and  $\eta \rightarrow \pi^+\pi^-\pi^0$ , respectively. The bin width of the histogram was chosen to be six times the resolution of the dark scalar particle, ensuring that the dark scalar particle predominantly appears in only one bin. For a conservative estimation, in the detector simulation, neutrons above the hit threshold of the EMC are all misidentified as photons. In the invariant mass distributions of  $e^+e^-$  and  $\pi^+\pi^-$ , no peaks are observed because the dark scalar particle has not been implemented in the

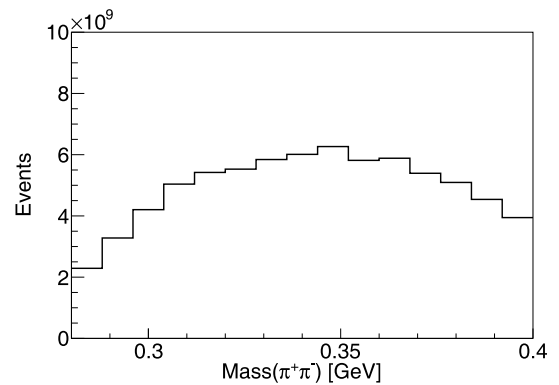


**Fig. 15.** Projected invariant mass distribution of  $\pi^+\pi^-$  in the channel  $\eta \rightarrow \pi^+\pi^-\pi^0$  for the suggested one-month running experiment.

GiBUU event generator. Consequently, the obtained invariant mass distributions represent only the background distributions, without the presence of the dark scalar particle. The lower the background distribution is, the better the sensitivity of the experiment will become.

### D. Branching-ratio upper limits

The invariant mass distributions of  $e^+e^-$  and  $\pi^+\pi^-$  present no bump, given that they are simply the background distributions without the presence of the dark scalar particle in the decay. Given that there is no signal peak in the distribution, the significance of dark scalar particles is less than  $3\sigma$ . With the background distribution after the event selection process, we can estimate the upper limit of the branching ratio for the dark scalar decay channel. The upper limit of the branching ratio for a new particle in the decay is simply given by

$$\text{Br. upper limit} = \frac{3 \times \sqrt{N_{\text{bg}}^i}}{N_\eta \times \epsilon_i}, \quad (4)$$

where  $N_{\text{bg}}^i$  is the resulting number of background events in bin  $i$ ,  $N_\eta$  is total number of  $\eta$  mesons produced in the

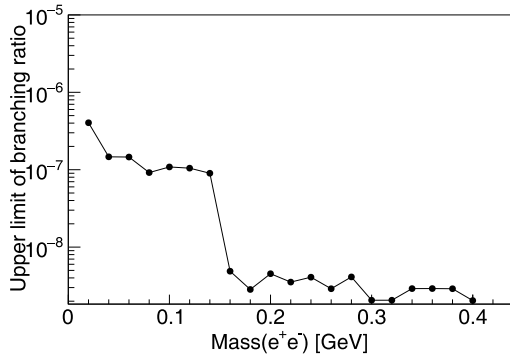


**Fig. 16.** Projected branching-ratio upper limit of dark scalar particles in the decay channel  $\eta \rightarrow S\pi^0 \rightarrow e^+e^-\gamma\gamma$  for the suggested one-month running experiment.

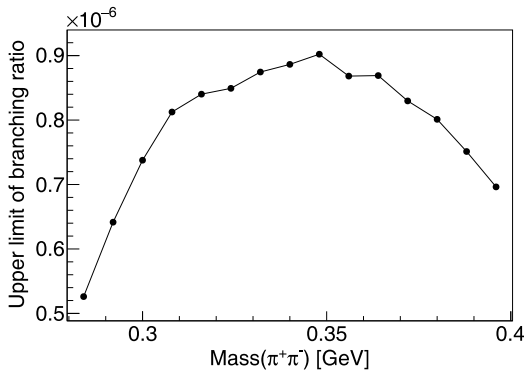


**Fig. 17.** Projected branching-ratio upper limit of dark scalar particles in the decay channel  $\eta \rightarrow S\pi^0 \rightarrow \pi^+\pi^-\gamma\gamma$  for the suggested one-month running experiment.

experiment, and  $\epsilon_i$  is the efficiency of detecting the dark scalar particle in the mass bin  $i$ . The confidence level is 99 % for the upper limit estimated using Eq. (4). The statistics for a total of  $\eta$  samples was discussed at the beginning of this section.

Figures 16 and 17 show the branching-ratio upper limits of a dark scalar particle in the decay as a function of the particle mass in the channels  $\eta \rightarrow S\pi^0 \rightarrow e^+e^-\gamma\gamma$  and  $\eta \rightarrow S\pi^0 \rightarrow \pi^+\pi^-\gamma\gamma$ , respectively. Figure 16 shows a fast decrease in the upper limit around 0.14 GeV. This is because most of the background electrons in the simulation originated from the decay of  $\pi^0$ . In the large mass region above the pion mass, the projected upper limit of dark scalar particles is close to  $10^{-9}$  in the  $e^+e^-$  channel. In the  $\pi^+\pi^-$  channel, the branching-ratio upper limit of dark scalar particles is below  $10^{-6}$ . Given that the direct  $\pi^+\pi^-\pi^0$  decay is one of the main decay channels of  $\eta$ , the upper limit of dark scalar particles given in this channel is not as small as expected.

### E. Sensitivities to model parameters

Applying the model description of the dark scalar particle in  $\eta$  rare decays, the upper limit of the branching ratio for  $\eta$  to dark scalar particles can be used to con-

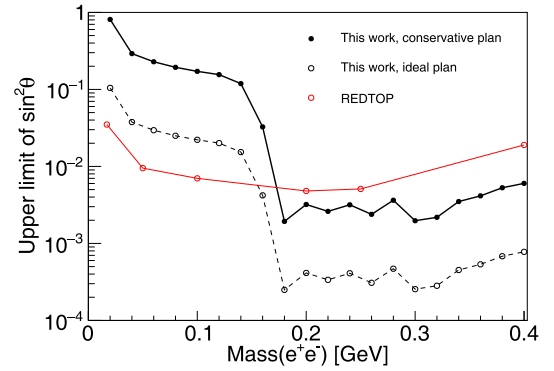


**Fig. 18.** (color online) Sensitivity to the parameter  $\sin^2\theta$  in the minimal scalar model as a function of the mass of the dark scalar particle for the suggested one-month running experiment (black solid curve, conservative plan). The projected sensitivity for an ideal case is also shown in the figure (black dashed curve). The ideal experimental plan is for a one-year run at an event rate of 500 MHz. The red dashed curve represents the preliminary result from the REDTOP experiment [35].

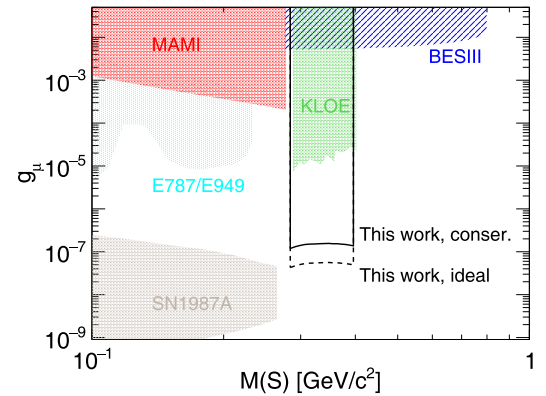


**Fig. 19.** (color online) Sensitivity to the parameter  $g_u$  in the hadrophilic scalar model as a function of the mass of the dark scalar particle for the suggested one-month running experiment (black solid curve, conservative plan). The projected sensitivity for an ideal case is also shown in the figure (black dashed curve). The ideal experimental plan is for a one-year run at an event rate of 500 MHz. Previous experimental data for the constraints were extracted from E787/E949 [70–73], MAMI [74], BESIII [52], KLOE [55], and SN 1987A [13, 75].

strain the free parameters in the model. The sensitivity to the model parameters refers to the precision with which we can test the model at a satisfactory significance level. In an experiment, the sensitivity to the model parameters is closely related to the measured upper limit of the branching ratio, as described by Eqs. (1) or (3).

Figure 18 shows the projected sensitivity of the mixing angle parameter as a function of the mass of the dark scalar particle according to the minimal scalar model. This sensitivity is based on the projected upper limit of



the branching ratio of  $\eta \rightarrow S\pi^0 \rightarrow e^+e^-\gamma\gamma$  for a prior one-month running experiment. Note that the sensitivity to  $\theta$  is approximately  $10^{-1}$  at a confidence level of 99%. The preliminary projection of REDTOP is also shown for comparison [35]. In the small-mass region, our results are worse than those of REDTOP, while in the large-mass region, our results are similar to those of REDTOP. Figure 18 also shows the sensitivity projection for an ideal one-year running experiment at an event rate of 500 MHz.

Figure 19 shows the projected sensitivity of the coupling parameter  $g_u$  as a function of the mass of dark scalar particle according to the hadrophilic scalar model. The sensitivity is based on the projected upper limit of the branching ratio of  $\eta \rightarrow S\pi^0 \rightarrow \pi^+\pi^-\gamma\gamma$  for a prior one-month running experiment. Note that the sensitivity to  $g_u$  is close to  $10^{-6}$  at a confidence level of 99%. Note that even with just one month of running for the proposed experiment, the sensitivity will surpass that of existing experiments in the corresponding mass domain. The current experimental constraints from MAMI and BESIII come from analyses of  $\eta \rightarrow \pi^0\gamma\gamma$  and  $\eta' \rightarrow \pi^0\pi^+\pi^-$  data, respectively, according to the same hadrophilic scalar model. Figure 19 also presents the sensitivity projection for an ideal experimental plan of one-year run at an event rate of 500 MHz. With years of running for the Huizhou  $\eta$  factory program, our constraints on the hadrophilic scalar model will be comparable to those of the proposed REDTOP experiment [35].

## VI. SUMMARY

A super  $\eta$  meson factory at Huizhou is proposed to explore new physics and precisely test the SM. The total number of  $\eta$  events for a preliminary one-month running experiment is estimated to be on the order of  $10^{11}$ , while the total number of inelastic scattering events is estimated to be on the order of  $10^{13}$ . The cross-section of  $\eta$  meson production in  $p$ - $A$  collisions is given by the GiBUU event generator.

To study the performance of the conceptual design of the spectrometer and investigate the physics impacts of the proposed experiments, we developed a simulation framework for the experiment. Both the signal ( $\eta \rightarrow$

$S\pi^0 \rightarrow e^+e^-\gamma\gamma$  and  $\eta \rightarrow S\pi^0 \rightarrow \pi^+\pi^-\gamma\gamma$ ) and background ( $\eta \rightarrow e^+e^-\gamma\gamma$  and  $\eta \rightarrow \pi^+\pi^-\gamma\gamma$ ) processes were simulated. The signal events for the dark scalar portal particle in  $\eta$  decay were generated using simple computer programs coded by us. The background events were generated with the GiBUU event generator. Additionally, we created a detector simulation tool, ChnsRoot, which is based on the FairRoot framework.

According to our simulations, the designed spectrometer has a large efficiency (approximately 40%) in collecting the events of interests ( $\eta \rightarrow S\pi^0 \rightarrow e^+e^-\gamma\gamma$  and  $\eta \rightarrow S\pi^0 \rightarrow \pi^+\pi^-\gamma\gamma$ ). Thanks to the small spatial resolution of the silicon pixel tracker, the invariant mass resolution of the dark scalar particle is excellent ( $< 2$  MeV) and the invariant mass resolution of  $\eta$  is acceptable ( $\sim 20$  MeV). The energy resolution of the photon should be improved in the future to further enhance the signal-to-background ratio. The branching-ratio upper limits of  $\eta \rightarrow S\pi^0 \rightarrow e^+e^-\gamma\gamma$  and  $\eta \rightarrow S\pi^0 \rightarrow \pi^+\pi^-\gamma\gamma$  were projected with our simulation framework. The branching-ratio upper limit of the dark scalar particle in the  $e^+e^-$  channel can reach  $10^{-9}$  in the larger mass region above the pion mass. The branching-ratio upper limit of the dark scalar particle in the  $\pi^+\pi^-$  channel is on the order of  $10^{-6}$ . The sensitivities to the parameters of the minimal scalar model and the hadrophilic model were obtained from the simulations as well.

In this simulation-based study of dark scalar sensitivities, the experimental uncertainties were not evaluated quantitatively. However, we provide basic information for estimating these uncertainties. The statistical uncertainty is expected to be notably small, as we plan to collect a large number of  $\eta$  meson samples at the Huizhou  $\eta$  factory. The systematic errors, which are related to the performance of the detectors, are anticipated to dominate the total experimental uncertainty. The systematic uncertainties for the sensitivity study mainly arise from the beam monitor, detection efficiency, particle misidentification, and momentum resolutions. Based on the results from current high-energy and nuclear experiments, these systematic uncertainties are under control and are expected to be at the level of several percentage points.

## References

- [1] B.-L. Young, *Front. Phys.* **12**, 121201 (2017), [Erratum: *Front. Phys.* **12**, 121202 (2017)]
- [2] A. Arbey and F. Mahmoudi, *Prog. Part. Nucl. Phys.* **119**, 103865 (2021), arXiv: 2104.11488[hep-ph]
- [3] E. Oks, *New Astron. Rev.* **93**, 101632 (2021), arXiv: 2111.00363[astro-ph.CO]
- [4] G. Bertone and T. M. P. Tait, *Nature* **562**, 51 (2018), arXiv: 1810.01668[astro-ph.CO]
- [5] T. Aramaki *et al.*, *Phys. Rept.* **618**, 1 (2016), arXiv: 1505.07785[hep-ph]
- [6] G. Lanfranchi, M. Pospelov, and P. Schuster, *Ann. Rev. Nucl. Part. Sci.* **71**, 279 (2021), arXiv: 2011.02157[hep-ph]
- [7] L. Gan, B. Kubis, E. Passemar *et al.*, *Phys. Rept.* **945**, 1 (2022), arXiv: 2007.00664[hep-ph]
- [8] B. Holdom, *Phys. Lett. B* **166**, 196 (1986)
- [9] P. Galison and A. Manohar, *Phys. Lett. B* **136**, 279 (1984)
- [10] P. Fayet, *Nucl. Phys. B* **347**, 743 (1990)
- [11] D. O'Connell, M. J. Ramsey-Musolf, and M. B. Wise, *Phys. Rev. D* **75**, 037701 (2007), arXiv: hep-ph/0611014
- [12] G. Krnjaic, *Phys. Rev. D* **94**, 073009 (2016), arXiv: 1505.07785[hep-ph]

- 1512.04119[hep-ph]
- [13] B. Batell, A. Freitas, A. Ismail *et al.*, *Phys. Rev. D* **100**, 095020 (2019), arXiv: 1812.05103[hep-ph]
- [14] B. Batell, A. Freitas, A. Ismail *et al.*, *Phys. Rev. D* **98**, 055026 (2018), arXiv: 1712.10022[hep-ph]
- [15] H. Georgi, D. B. Kaplan, and L. Randall, *Phys. Lett. B* **169**, 73 (1986)
- [16] D. Gorbunov and M. Shaposhnikov, *JHEP* **10**, 015 (2007)
- [17] L. Zhao and J. Liu, *Front. Phys. (Beijing)* **15**, 44301 (2020), arXiv: 2004.04547[astro-ph.IM]
- [18] J. Liu, X. Chen, and X. Ji, *Nature Phys.* **13**, 212 (2017), arXiv: 1709.00688[astro-ph.CO]
- [19] S. Cebrián, *J. Phys. Conf. Ser.* **2502**, 012004 (2023), arXiv: 2205.06833[physics.ins-det]
- [20] N. Du *et al.* (ADMX), *Phys. Rev. Lett.* **120**, 151301 (2018), arXiv: 1804.05750[hep-ex]
- [21] Z. Y. Zhang *et al.* (CDEX), *Phys. Rev. Lett.* **132**, 171001 (2024), arXiv: 2309.14982[hep-ex]
- [22] Y. Hochberg, Y. F. Kahn, R. K. Leane *et al.*, *Nature Rev. Phys.* **4**, 637 (2022)
- [23] I. Georgescu, *Nature Rev. Phys.* **4**, 216 (2022)
- [24] O. Buchmueller, C. Doglioni, and L. T. Wang, *Nature Phys.* **13**, 217 (2017), arXiv: 1912.12739[hep-ex]
- [25] M. Felcini (ATLAS, CMS), arXiv: 1809.06341 [hep-ex]
- [26] G. Jungman, M. Kamionkowski, and K. Griest, *Phys. Rept.* **267**, 195 (1996), arXiv: hep-ph/9506380
- [27] G. Bertone, D. Hooper, and J. Silk, *Phys. Rept.* **405**, 279 (2005), arXiv: hep-ph/0404175
- [28] J. L. Feng, *Ann. Rev. Astron. Astrophys.* **48**, 495 (2010), arXiv: 1003.0904[astro-ph.CO]
- [29] S. Navas *et al.* (Particle Data Group), *Phys. Rev. D* **110**, 030001 (2024)
- [30] L. Roszkowski, E. M. Sessolo, and S. Trojanowski, *Rept. Prog. Phys.* **81**, 066201 (2018), arXiv: 1707.06277[hep-ph]
- [31] S. R. Golwala *et al.* (CDMS), *Nucl. Instrum. Meth. A* **444**, 345 (2000)
- [32] M. Pospelov, A. Ritz, and M. B. Voloshin, *Phys. Lett. B* **662**, 53 (2008), arXiv: 0711.4866[hep-ph]
- [33] M. Pospelov and A. Ritz, *Phys. Lett. B* **671**, 391 (2009), arXiv: 0810.1502[hep-ph]
- [34] N. Baltzell *et al.*, arXiv: 2203.08324 [hep-ex]
- [35] J. Elam *et al.* (REDTOP), arXiv: 2203.07651 [hep-ex]
- [36] A. J. Krasznahorkay *et al.*, *Phys. Rev. Lett.* **116**, 042501 (2016), arXiv: 1504.01527[nucl-ex]
- [37] D. P. Aguillard *et al.* (Muon g-2), *Phys. Rev. Lett.* **131**, 161802 (2023), arXiv: 2308.06230[hep-ex]
- [38] B. Abi *et al.* (Muon g-2), *Phys. Rev. Lett.* **126**, 141801 (2021), arXiv: 2104.03281[hep-ex]
- [39] J. P. Miller, E. de Rafael, and B. L. Roberts, *Rept. Prog. Phys.* **70**, 795 (2007), arXiv: hep-ph/0703049
- [40] J. L. Feng, B. Fornal, I. Galon *et al.*, *Phys. Rev. Lett.* **117**, 071803 (2016), arXiv: 1604.07411[hep-ph]
- [41] J. L. Feng, B. Fornal, I. Galon *et al.*, *Phys. Rev. D* **95**, 035017 (2017), arXiv: 1608.03591[hep-ph]
- [42] C. Cazzaniga *et al.* (NA64), *Eur. Phys. J. C* **81**, 959 (2021), arXiv: 2107.02021[hep-ex]
- [43] A. Bodas, R. Coy, and S. J. D. King, *Eur. Phys. J. C* **81**, 1065 (2021), arXiv: 2102.07781[hep-ph]
- [44] T. Nomura and P. Sanyal, *JHEP* **05**, 232 (2021), arXiv: 2010.04266[hep-ph]
- [45] A. Ariga *et al.* (FASER), *Phys. Rev. D* **99**, 095011 (2019), arXiv: 1811.12522[hep-ph]
- [46] J. Prentki and M. J. G. Veltman, *Phys. Lett.* **15**, 88 (1965)
- [47] M. Ablikim *et al.* (BESIII), *Phys. Rev. D* **87**, 012009 (2013), arXiv: 1209.2469[hep-ex]
- [48] M. Ablikim *et al.* (BESIII), *Phys. Rev. D* **107**, 092007 (2023), arXiv: 2302.08282[hep-ex]
- [49] M. Ablikim *et al.* (BESIII), *Phys. Rev. D* **92**, 012014 (2015), arXiv: 1506.05360[hep-ex]
- [50] M. Ablikim *et al.* (BESIII), *Phys. Rev. D* **87**, 032006 (2013), arXiv: 1211.3600[hep-ex]
- [51] M. Ablikim *et al.* (BESIII), *Phys. Rev. Lett.* **112**, 121201 (2014), [Erratum: *Phys. Rev. Lett.* **113**, 039903 (2017)], arXiv: 1404.0096 [hep-ex]
- [52] M. Ablikim *et al.* (BESIII), *Phys. Rev. Lett.* **118**, 012001 (2017), arXiv: 1606.03847[hep-ex]
- [53] W. Krzemien and E. Pérez del Río (KLOE-2), *Int. J. Mod. Phys. A* **34**, 1930012 (2019), arXiv: 1909.01233[hep-ex]
- [54] D. Babusci *et al.* (KLOE-2), *JHEP* **10**, 047 (2020), arXiv: 2006.14710[hep-ex]
- [55] A. Anastasi *et al.* (KLOE-2), arXiv: 1601.06985[hep-ex]
- [56] F. Ambrosino *et al.* (KLOE), *Phys. Lett. B* **675**, 283 (2009), arXiv: 0812.4830[hep-ex]
- [57] X.-R. Chen *et al.*, arXiv: 2407.00874 [hep-ph]
- [58] C. P. Burgess, M. Pospelov, and T. ter Veldhuis, *Nucl. Phys. B* **619**, 709 (2001), arXiv: hep-ph/0011335
- [59] F. Piazza and M. Pospelov, *Phys. Rev. D* **82**, 043533 (2010), arXiv: 1003.2313[hep-ph]
- [60] C. Kouvaris, I. M. Shoemaker, and K. Tuominen, *Phys. Rev. D* **91**, 043519 (2015), arXiv: 1411.3730[hep-ph]
- [61] B. Patt and F. Wilczek, arXiv: hep-ph/0605188
- [62] B. Batell, M. Pospelov, and A. Ritz, *Phys. Rev. D* **80**, 095024 (2009), arXiv: 0906.5614[hep-ph]
- [63] J. L. Feng, I. Galon, F. Kling *et al.*, *Phys. Rev. D* **97**, 055034 (2018), arXiv: 1710.09387[hep-ph]
- [64] F. Bezrukov and D. Gorbunov, arXiv: 1303.4395[hep-ph]
- [65] O. Buss, T. Gaitanos, K. Gallmeister *et al.*, *Phys. Rept.* **512**, 1 (2012), arXiv: 1106.1344[hep-ph]
- [66] T. Gaitanos, H. Lenske, and U. Mosel, *Phys. Lett. B* **663**, 197 (2008), arXiv: 0712.3292[nucl-th]
- [67] J. Weil, H. van Hees, and U. Mosel, *Eur. Phys. J. A* **48**, 111 (2012), [Erratum: *Eur. Phys. J. A* **48**, 150 (2012)], arXiv: 1203.3557 [nucl-th]
- [68] M. Al-Turany, D. Bertini, R. Karabowicz *et al.*, *J. Phys. Conf. Ser.* **396**, 022001 (2012)
- [69] C. Wilkin, *Eur. Phys. J. A* **53**, 114 (2017), arXiv: 1611.07250[nucl-ex]
- [70] S. Adler *et al.* (E787), *Phys. Lett. B* **537**, 211 (2002), arXiv: hep-ex/0201037
- [71] S. Adler *et al.* (E787), *Phys. Rev. D* **70**, 037102 (2004), arXiv: hep-ex/0403034
- [72] S. Adler *et al.* (E949, E787), *Phys. Rev. D* **77**, 052003 (2008), arXiv: 0709.1000[hep-ex]
- [73] A. V. Artamonov *et al.* (BNL-E949), *Phys. Rev. D* **79**, 092004 (2009), arXiv: 0903.0030[hep-ex]
- [74] Y.-S. Liu, I. C. Cloët, and G. A. Miller, *Nucl. Phys. B*, 114638 (2019), arXiv: 1805.01028[hep-ph]
- [75] E. Hardy, A. Sokolov, H. Stubbs, arXiv: 2410.17347 [hep-ph]